Available online at www.sciencedirect.com
ScienceDirect
Journal of the European Ceramic Society 27 (2007) 3727–3730
www.elsevier.com/locate/jeurceramsoc

Far infrared reflection spectroscopy of Zn_2SnO_4 ceramics obtained by sintering mechanically activated ZnO–SnO_2 powder mixtures

M.V. Nikolić [a,*], T. Ivetić [b], K.M. Paraskevopoulos [c], K.T. Zorbas [c], V. Blagojević [d], D. Vasiljević-Radović [e]

[a] *Center for Multidisciplinary Studies of the University of Belgrade, Kneza Višeslava 1, 11000 Belgrade, Serbia*
[b] *Institute of Technical Sciences of SASA, Knez Mihailova 35, 11000 Belgrade, Serbia*
[c] *Solid State Section, Physics Department, Aristotle University, 52124 Thessaloniki, Greece*
[d] *Faculty of Electronic Engineering, Bul. Kralja Aleksandra 72, 11000 Belgrade, Serbia*
[e] *Institute of Microelectronics & Single Crystals, Njegoševa 12, 11000 Belgrade, Serbia*

Available online 9 March 2007

Abstract

A mixture of starting ZnO and SnO_2 powders (molar ratio 2:1) were mechanically activated for 10, 40, 80 and 160 min in a planetary ball mill and then isothermally sintered at 1300 °C for 2 h in order to obtain Zn_2SnO_4 ceramics. X-ray diffraction analysis confirmed single-phase polycrystals. Far infrared reflection spectra were measured (100–1400 cm^{-1}). The same oscillators were observed, but the highest intensity of reflectivity peaks was obtained for the powder activated 10 min and it gradually decreased with longer times of mechanical activation. This is in agreement with microstructure analysis where longer times of mechanical activation lead to increased porosity and defects. Using group theory six ionic oscillators were calculated for single crystal Zn_2SnO_4 spectra, but two more oscillators were observed in the obtained experimental spectra, which could be the result of mechanical activation and sintering. The FIR experimental results were numerically analyzed and oscillator parameters were calculated.

Keywords: Milling; Sintering; Spectroscopy; Optical properties; Spinels

1. Introduction

Zinc-stannate is a low cost and non-toxic transparent material best known for its gas sensing properties,[1] though a lot of research has been devoted to possible applications as thin film devices.[2,3] Integration of zinc-stannate thin films into a CdS/CdTe solar cell as a buffer resulted in improved device performance.[4] Synthesis of single crystal nanobelts, nanorings and nanocones has also been investigated.[5,6]

Mechanical activation by grinding is widely used in powder processing.[7] Synthesis of polycrystalline zinc-stannate by a solid-state reaction and the influence of mechanical activation on its formation were studied in detail by Nikolic et al.[8,9] In this work we have studied optical properties of Zn_2SnO_4 ceramics obtained by sintering ZnO–SnO_2 powder mixtures that were mechanically activated for different activation times.

2. Experimental

Commercial ZnO and SnO_2 powders (Aldrich) in the molar ratio 2:1 were mechanically activated in a planetary ball mill (Fritsch Pulversette 5) in a continuous grinding regime in air for 10, 40, 80 and 160 min. The powder to balls (zirconium oxide, approx. 10 mm in diameter) ratio was 40:1. The powders obtained were uniaxially pressed with 980 MPa into discs 10 mm in diameter and then sintered at 1300 °C for 2 h.

X-ray analysis of the obtained sintered samples was conducted on an X-ray diffractometer (Norelco-Philips PW-1050) with Cu Kα radiation and a step scan mode of 0.02°/0.4 s. Microstructural characterization was carried out using a scanning electron microscope JEOL JSM 6460 LV.

Room temperature far infrared optical reflectivity measurements were performed using normal incidence light in the range between 100 and 1400 cm^{-1} using a Brucker 113V FTIR spectrometer. Prior to measuring the samples were highly polished first with silicone carbide P1000 and P1500 sandpaper and then with 3 μm grade diamond paste.

* Corresponding author. Tel.: +381 11 637 367; fax: +381 11 185263.
E-mail address: maria@mi.sanu.ac.yu (M.V. Nikolić).

0955-2219/$ – see front matter © 2007 Elsevier Ltd. All rights reserved.
doi:10.1016/j.jeurceramsoc.2007.02.040

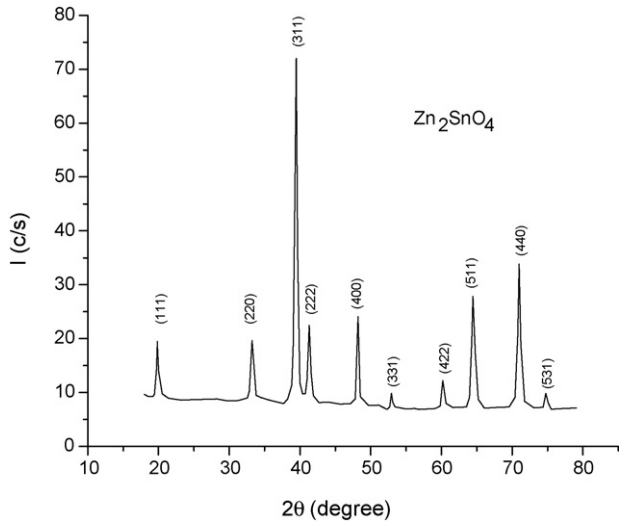

Fig. 1. X-ray diffraction spectra of Zn_2SnO_4 obtained by mechanical activation for 160 min followed by sintering.

3. Results and discussion

X-ray diffraction analysis of all Zn_2SnO_4 samples mechanically activated for different activation times (10, 40, 80 and 160 min) and then sintered showed that they were all polycrystalline with peaks characteristic for spinel zinc-stannate. An example is given in Fig. 1 for the Zn_2SnO_4 sample mechanically activated for 160 min.

The reflectivity of near normal incidence light in the range measured as a function of the wave number is given in Fig. 2 for all analyzed Zn_2SnO_4 samples (in the range between 100 and 1000 cm^{-1} containing all relevant changes). One can see that regardless of the time of mechanical activation all samples showed the existence of the same peaks (oscillators), though their intensity was different. The highest intensity of reflectivity peaks was obtained for the powder activated for 10 min and it gradually decreased with longer times of mechanical activation.

Previous research of mechanically activated Zn_2SnO_4 powders before sintering showed that formation of a spinel zinc-stannate phase started after 40 min of activation, while the

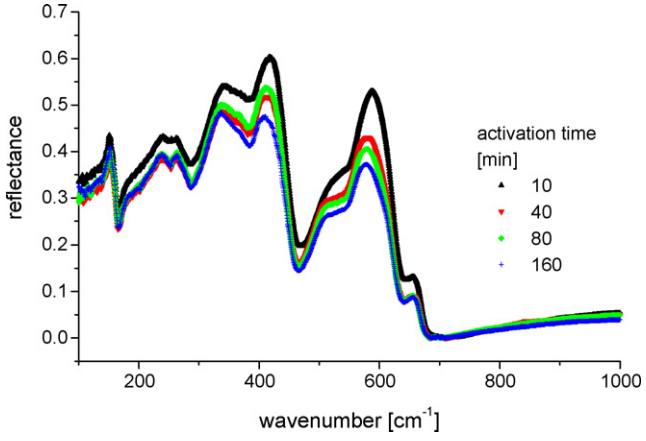

Fig. 2. IR spectra of Zn_2SnO_4 obtained by mechanical activation for 10, 40, 80 and 160 min followed by sintering.

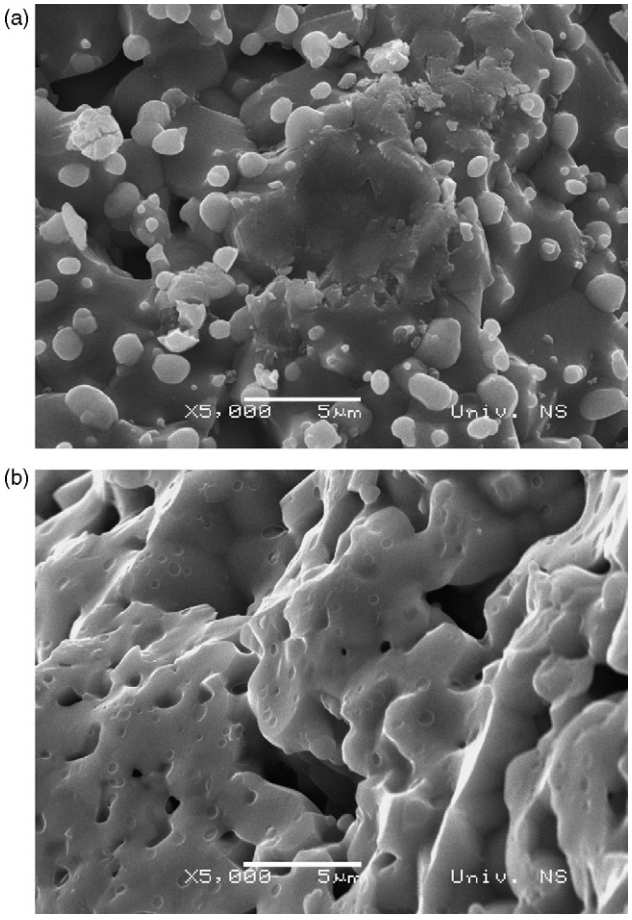

Fig. 3. SEM fractured surface of Zn_2SnO_4 obtained by mechanical activation for 10 min (a) and 40 min (b) followed by sintering.

powder activated for 10 min showed a significant refinement in crystallite size of the initial oxides.[9] Agglomeration and a high porosity were present in all mechanically activated powders that increased with longer times of mechanical activation and remained after sintering.[10] An analysis of the density of the mechanically activated samples after sintering showed that the sample activated for 10 min had a slightly higher density (activation times: 10–75.9, 40–75.7, 80–75.5 and 160–75.3% of the theoretical density).[10] Changes in the microstructure for different activation times can be seen in Fig. 3 showing SEM fractured surfaces of zinc-stannate mechanically activated for 10 and 40 min and sintered.

Zn_2SnO_4 has an inverse cubic spinel structure with a face-centered cubic unit cell (space group $Fd\bar{3}m$ or O_h^7). Segev and Wei[11] studied the cation distribution in spinel oxides including zinc-stannate. They proved zinc-stannate stable in the inverse spinel structure by determining the cubic lattice constant to be $a = 8.658$ Å, anion displacement parameter $u = 0.3833$ and cation inversion parameter $x = 1$, with inverse energy $\Delta E = -0.64$ eV/molecule. Thus, Zn^{2+} atoms occupy tetrahedral voids and Zn^{2+} and Sn^{4+} atoms randomly occupy the octahedral voids. Using nuclear site group analysis[12] and taking into account the position of the atoms in the unit cell of zinc-stannate (Wyckoff sites, ICSD Code 28235) that are 8*a* and

16*d* for zinc atoms, 16*d* for tin atoms and 32*e* for oxygen atoms, one can calculate the total number of active and inactive IR and Raman modes. For zinc-stannate we calculated:

$$\Gamma = 1A_{1g} + 1E_g + 3F_{2g} + 7F_{1u}$$

where A_{1g}, E_g and F_{2g} represent the active Raman modes and F_{1u} represent infrared modes. As one IR mode is inactive, there are 6IR active infrared modes.

Numerical analysis of the measured IR spectra was performed using a four-parameter model of coupled oscillators first introduced by Gervais and Piriou[13] defining the factorized form of the dielectric function as:

$$\varepsilon = \varepsilon_1 \pm j\varepsilon_2 = \varepsilon_\infty \prod_j \frac{\omega_{j\mathrm{LO}}^2 - \omega^2 + i\gamma_{j\mathrm{LO}}\omega}{\omega_{j\mathrm{TO}}^2 - \omega^2 + i\gamma_{j\mathrm{TO}}\omega} \quad (1)$$

where $\omega_{j\mathrm{TO}}$ and $\omega_{j\mathrm{LO}}$ are transverse (TO) and longitudinal (LO) frequencies, $\gamma_{j\mathrm{TO}}$ and $\gamma_{j\mathrm{LO}}$ are transverse and longitudinal damping factors, respectively, while ε_∞ is the high frequency dielectric permittivity contribution.

In order to obtain starting values for the four-parameter model the reflectivity diagrams were first analyzed using the Kramers–Kronig method. These values were then used in the numerical analysis with a program package developed in FORTRAN 95 enabling separate or simultaneous fitting of all parameters.

For all samples eight coupled oscillators of varied strength were determined. An example of the good agreement obtained between the experimental and calculated curves is given in Fig. 4. The values obtained for the high frequency dielectric contribution, transverse and longitudinal frequencies and damping factors are given in Table 1. Compared to the theoretical prediction, we have obtained two more oscillators. These two oscillators originate from the defective nature of the spinel lattice[14]. In this case this is the result of mechanical activation followed by sintering resulting in a structure containing pores, aggregates and intergranular materials besides crystalline grains. There is little literature data on IR spectra of zinc-stannate. Porotnikov et al.[15] determined 7IR (159, 266, 380, 430, 535, 575 and 650 cm^{-1}) modes using infrared transmission spectroscopy for two forms of zinc-stannate. A careful analysis of the measured IR spectra and the values given in Table 1 show that 6 of the 8IR modes we determined for zinc-stannate are in accordance with 6 of the 7IR values obtained by Porotnikov et al.[15] enabling determination of the two extra oscillators (marked with * in Table 1).

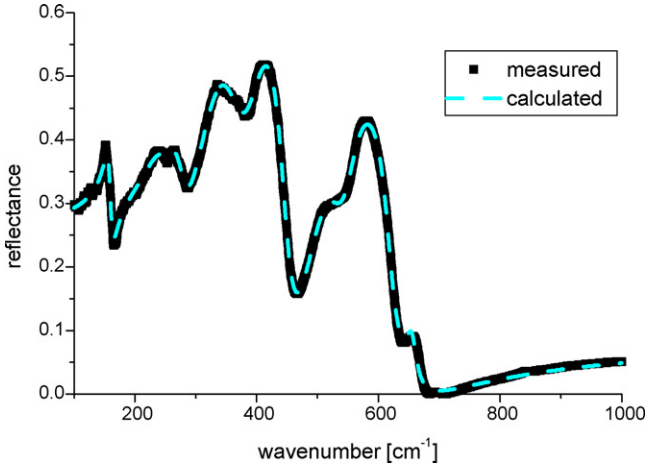

Fig. 4. Measured (points) and calculated (dotted line) far infrared reflectivity curves for Zn_2SnO_4 mechanically activated for 40 min.

Table 1
Parameter values determined for Zn_2SnO_4 obtained by mechanical activation of starting powders followed by sintering

Oscillators	Parameters	Activation time			
		10	40	80	160
	ε_∞	3.2	3.3	3.2	2.9
I	ω_{TO1}	155.7	156.6	156.9	155.7
	γ_{TO1}	14.3	12.7	13.4	15.1
	ω_{LO1}	160.4	160.8	161.5	161.4
	γ_{LO1}	11.7	11.3	11.4	12.9
II*	ω_{TO2}	252.8	252.8	252.3	252.4
	γ_{TO2}	74.8	47.1	48.7	49.4
	ω_{LO2}	253.8	253.7	252.9	252.0
	γ_{LO2}	28.5	30.2	29.5	25.6
III	ω_{TO3}	257.9	262.4	262.9	260.4
	γ_{TO3}	33.5	38.4	41.3	39.1
	ω_{LO3}	285.1	279.5	282.1	281.2
	γ_{LO3}	46.2	38.2	35.6	32.2
IV	ω_{TO4}	321.9	326.4	321.4	315.1
	γ_{TO4}	60.3	65.0	63.4	68.4
	ω_{LO4}	375.1	374.3	378.1	380.1
	γ_{LO4}	60.4	67.0	67.7	68.6
V	ω_{TO5}	391.5	396.8	396.7	397.9
	γ_{TO5}	60.9	62.8	56.5	59.4
	ω_{LO5}	451.2	450.8	449.6	449.1
	γ_{LO5}	36.0	37.1	36.8	42.3
VI*	ω_{TO6}	484.2	495.7	495.2	495.7
	γ_{TO6}	98.9	78.9	79.4	83.5
	ω_{LO6}	559.7	539.8	539.9	541.4
	γ_{LO6}	86.5	53.7	55.2	56.3
VII	ω_{TO7}	563.1	550.4	550.9	551.7
	γ_{TO7}	61.1	49.5	50.0	49.9
	ω_{LO7}	620.7	618.7	619.4	619.3
	γ_{LO7}	22.3	29.1	33.7	37.1
VIII	ω_{TO8}	654.1	654.1	658.2	658.2
	γ_{TO8}	29.8	33.7	31.5	25.8
	ω_{LO8}	655.6	655.8	659.3	659.3
	γ_{LO8}	12.1	14.4	13.3	11.9

Porotnikov et al.[15] assigned the modes between 150 and 420 cm^{-1} to be characteristic for Zn–O bonds, while the higher frequency modes between 550 and 650 cm^{-1} are characteristic for Sn–O bonds. According to Lutz et al.[16] all allowed IR modes represent typical lattice vibrations with contributions of all atoms and all bonds of the spinel structure. However, some bands can be more affected by the nature of the octahedrally coordinated metals or the metals on the tetrahedral sites and thus the higher frequency modes of Zn_2SnO_4 are more affected by the nature of Sn cations on octahedral sites and the lower frequency modes are more affected by Zn cations on both octahedral and tetrahedral sites.

4. Conclusion

Room temperature far infrared spectra were measured of Zn_2SnO_4 samples obtained by mechanical activation of the starting powders for different times of activation (10, 40, 80 and 160 min) followed by sintering. Eight ionic oscillators were determined and numerically analyzed for all samples. The intensity of reflectivity peaks was the highest for the sample activated 10 min and decreased with the duration of mechanical activation. This is in accordance with microstructure analysis performed where longer times of activation lead to increasing porosity and defects. The two extra oscillators from the six determined by nuclear site group analysis and known Wyckoff sites for zinc-stannate were identified and are the result of mechanical activation and sintering.

Acknowledgements

The authors would like to express their gratitude to Acad. M.M. Ristić and Acad. P.M. Nikolić for useful discussions. We are also grateful to the Greek Secretariat of Research and Development for partial support under the bileteral program between Serbia and Greece. This work was performed as part of projects 142011G and 6150B financed by the Ministry for Science and Environmental Protection of the Republic of Serbia.

References

1. Yu, J. H. and Choi, G. M., Selective CO gas detection of Zn_2SnO_4 gas sensor. *J. Electroceram.*, 2003, **8**, 249–255.
2. Coutts, T. J., Young, D. L., Li, X., Mullingan, W. P. and Wu, X., Search for improved transparent conducting oxides: A fundamental investigation of CdO, Cd_2SnO_4 and Zn_2SnO_4. *J. Vac. Sci. Technol. A*, 2000, **18**, 2646–2660.
3. Young, D. L., Williamson, D. L. and Coutts, T. J., Structural characterization of zinc-stannate thin films. *J. Appl. Phys.*, 2001, **91**, 1464–1471.
4. Wu, X., Asher, S., Levi, D. H., King, D. E., Yan, Y., Gessert, T. A. and Sheldon, P., Interdiffusion of CdS and Zn_2SnO_4 layers and its application in CdS/CdTe polycrystalline thin-film solar cells. *J. Appl. Phys.*, 2001, **89**, 4564–4569.
5. Wang, J. X., Xie, S. S., Yuan, H. J., Dan, X. Q., Liu, D. F., Gao, Y., Zhou, Z. P., Song, L., Liu, L. F., Zhao, X. W., Dou, X. Y., Zhou, W. Y. and Wang, G., Synthesis, structure and photoluminescence of Zn_2SnO_4 single-crystal nanobelts and nanorings. *Solid State Commun.*, 2004, **131**, 435–440.
6. Li, Y. and Ma, X. L., Nanobelts and nanocones of spinel Zn_2SnO_4. *Phys. Stat. Sol.*, 2005, **202**, 435–440.
7. Zhang, D. L., Processing of advanced materials using high-energy mechanical milling. *Prog. Mater. Sci.*, 2004, **49**, 537–560.
8. Nikolić, N., Srećković, T. and Ristić, M. M., The influence of mechanical activation on zinc-stannate spinel formation. *J. Eur. Ceram. Soc.*, 2001, **21**, 2071–2074.
9. Nikolic, N., Marinkovic, Z. and Sreckovic, T., The influence of grinding conditions on the mechanochemical synthesis of zinc-stannate. *J. Mater. Sci.*, 2004, **39**, 5239–5242.
10. Ivetic, T., MSc thesis, Belgrade, 2006 (in Serbian).
11. Segev, D. and Wei, S.-H., Structure-derived electronic and optical properties of transparent conducting oxides. *Phys. Rev. B*, 2005, **71**, 125–129.
12. Rousseau, D. L., Bauman, R. P. and Porto, S. P. S., Normal mode determination in crystals. *J. Raman Spectrosc.*, 1981, **10**, 253–290.
13. Gervais, F. and Piriou, B., Temperature dependence of transverse and longitudinal-optic modes in TiO_2 (rutile). *Phys. Rev. B*, 1974, **10**, 1642–1654.
14. Thibaudeau, P. and Gervais, F., Ab initio investigation of phonon modes in the $MgAl_2O_4$ spinel. *J. Phys.: Condens. Matter*, 2002, **14**, 3543–3552.
15. Porotnikov, N. V., Savenko, V. G. and Sidorova, O. V., Kolebatelnie spektri shpineley sostava Zn_2SnO_4 i Mg_2SnO_4. *Zh. Neorg Khimii*, 1983, **28**, 1653–1655;
    Porotnikov, N. V., Savenko, V. G. and Sidorova, O. V., Kolebatelnie spektri shpineley sostava Zn_2SnO_4 i Mg_2SnO_4. *Rus. J. Inorg. Chem.*, 1983, **28**, 983–985.
16. Lutz, H. D., Mueller, B. and Steiner, H. J., Lattice vibration spectra. LIX. Single crystal infrared and Raman studies of spinel type oxides. *J. Solid State Chem.*, 1991, **90**, 54–60.